Sensors & Transducers, Vol. 180, Issue 10, October 2014, pp. 156-165

www.sensorsportal.com

Sensors & Transducers

© 2014 by IFSA Publishing, S. L.
http://www.sensorsportal.com

A Case Study of the Seasonal Underground Variation Contributions to the gPhone Gravimeter Observations Based on Fourier Analysis

[1, 2, 3] Wei Jin, [2, 3] Li Hui, [1] Shen Wenbin

[1] School of Geodesy and Geomatics ,Wuhan University, Wuhan 430079, China
[2] Institute of Seismology, CEA, Wuhan 430071, China
[3] Crustal Movement Laboratory, Wuhan 430071, China
[1] Tel.: 15927365563
E-mail: pierce212@163.com

Received: 2 July 2014 /Accepted: 30 September 2014 /Published: 31 October 2014

Abstract: In this paper, the seasonal gravity variation rules of gPh040 continuous gravity visualizer in Wujiahe seismic station caused by underground water variation was obtained with the Fourier series analysis method and polynomial fitting method using the continuous gravity observation data of this kind of gravimeter within the period of two and a half years. The result shows that the observation accuracy of gPh040 can reach up to 50 % of the accuracy of superconductive gravimeter in the noise level of approximately $\pm 0.3\times10^{-8}$ ms^{-2}/cm. The seasonal underground water contributions can be well obtained by both of the two methods compared with the actual measurement of underground water variation and the global water model (the correlation coefficient of above 80 %). And the correlation coefficient between drift correction method of Fourier analysis and actual measurement of underground water level is as high as 95 %. The impact factor (0.153×10^{-8} ms^{-2}/cm) of underground water level variation to gravity calculated by this method is near the theoretical result of physical ground measurement. Therefore, comparing with the polynomial fitting method, the Fourier analysis method can not only fit a better continuous drift of spring gravimeter but also provide a new analysis way to contrast the contribution of seasonal underground variation to the gPhone type continuous gravity observation. *Copyright © 2014 IFSA Publishing, S. L.*

Keywords: gPhone040, GLDAS, CPC, Underground water, Fourier analysis.

1. Introduction

Continuous gravity observation is able to detect the long-term (years) and short-term (seasons) variation of superposed gravity change effects, which is caused by the migration of various materials in earth system [1]. The gravity change effects mainly consist of self-changes of hydrology, atmosphere, earth and ocean tides, etc, and the materials migration process of earth crust deformation in earth system and structure changes caused by its loads [1-5]. To collect long-term signals, spring and superconductive gravimeter must face the interference of drift in effective signal. Van Camp and Francis (2007) [6] studied the drift characteristic of superconductive gravimeter with absolute gravimeter, and they pointed out that the drift of gravimeter could be confirmed by the same site observation of absolute gravimeter and superconductive gravity gravimeter. Riccardi et al (2011) [7] researched the drift characteristic of gPhone gravimeter using polynomial fitting method by comparison and measurement of gPhone054 spring gravimeter and GWRC026, although the observation data of gravimeter

especially the spring gravimeter could be interrupted in the actual observation by the interference of external factors such as power failure and lighting stroke, eventually the complexity of segmentation fitting would be increased and the observation data could not be used at all. The research team of Institute of Seismology in China Seismological Bureau [8] studied the observation data of seven gPhone gravimeters in the digital earthquake observation network using segmentation fitting drift method, and proposed the contribution of underground water variation to gravity field.

This work is based on the observation data of gPhone gravimeter in Wujiahe seismic station during the years of 2008~2011 in the digital earthquake observation network. The spring gravimeter drift is confirmed and the gravity variation signals caused by seasonal variation of underground water are quantitatively contrasted using a new analysis method with comprehensive consideration of air pressure and underground water level monitor tools of this station, with constraint of global land water model, and with combination of spring type gravimeter drift continuity and the continuity characteristics of gravity variation.

2. Fourier Analysis of Solid Earth Tides Observation Data

Although there is a lot of complexity as to the spring gravimeter drift, the drift is a continuous process without the obvious interference of external factors (measurement break down, serous lighting stroke, long term failure due to power cut, etc.) to spring [9]. The superimposed gravity variation caused by external factors should also be a continuous process. Therefore, considering that any of continuous periodic function could be unfolded as Fourier series, this work simulated and observed the complex and continuous drift using the Fourier analysis method. The non-tidal analysis model and drift error function simulated by Fourier series are as follows:

$$g_{gPhone} = g_{tide+ocean} + g_{nontidel} + g_{drift} + \varepsilon, \quad (1)$$

$$g_{nontide} = g_{air} + g_{pol} + g_{waterload} + \varepsilon_1, \quad (2)$$

$$g_{drift}(t_i) = a_0 + \sum_{j=1}^{n} (a_j \cos \omega_0 n t_i + b_j \sin \omega_0 n t_i) + \varepsilon_2, \quad (3)$$

In equation (1), the gravity observation data g_{gPhone} is mainly consist of tidal part g_{tide}, non-tidal part $g_{nontide}$, the drift g_{drift}, and the error ε. In equation (2), the non-tidal part $g_{nontide}$ is mainly resulted from the pole-shift tide g_{pol} and the migration contribution of seasonal materials, such as air pressure load g_{air}, water load $g_{waterload}$, and non-tidal noise ε_1. Equation (3) adopts the truncated form of infinite series (up to n order), where g_{drift} is the drift of meter, a_j and b_j $(j = 1,2,3\ldots,n)$ are the fitting parameter of Fourier series, n is the order of Fourier series, t_i $(i = 0,1,2,3,\ldots,m)$ is the observation time, the subscript i represents for the observation time counted as i, m is the total observation data numbers, and ω_0 is the angular speed which is usually calculated by $\pi/(m-1)$.

Given a drift time sequence, the Fourier series fitting parameter a_j, b_j $(j = 1,2,3\ldots,n)$ can be resolved using error function equation (3) and the least squares principle, thus the drift rules of observation time sequence can be confirmed.

3. Handling and Analyzing of Observation Data in Wujiahe Seismic Station

3.1. Station and Observation Data

In the year of 2007, 17 gPhone type of spring gravimeter was induced from LRC Corporation U.S.A. by China Seismological Bureau. The continuous observation and measurement was performed in Joufeng seismic station in Wuhan Hubei Province. The gravimeter was calibrated using the M_2 wave tidal factor measured by the superconducting gravimeter SGC053 in this station in 2010. The calibration factor of gPhone040 (gPh040 for short below) spring gravimeter was 1.0024×10^{-8} ms^{-2}/V. After the measurement, the gPh040 spring gravimeter was installed in the cave of Wujiahe seismic station in Nei Monggol Autonomous Region in 2007. The north of this cave was Yin Mountain, and the south was wide Hetao impact plain. It had drought in nine years out of tem. The station provided not only the assistant observation of air and water pressure and rainfall, but also the observation station of underground water level in the mountain 800 miles away far from the seismic station. After the test run, gPh040 has been working regularly since Sep. 2008. Although a small time of power cut and failure happened during the observation process, the meter could work stable on the whole. The data sample interval of gPh040 is 1 Hz.

3.2. Data Pre-processing

It is shown in Fig. 1 that the main factor which influents the spring gravimeter is the irregular drift of spring beside the solid earth tide. At the same time, the anisotropy of the spring itself leads to the difficulty of accurate simulation of spring drift using fixed mathematical function. Finally, the micro-gal level effect caused by external factors would be covered up of by solid earth tide, and what's more, flooded by the spring gravimeter drift.

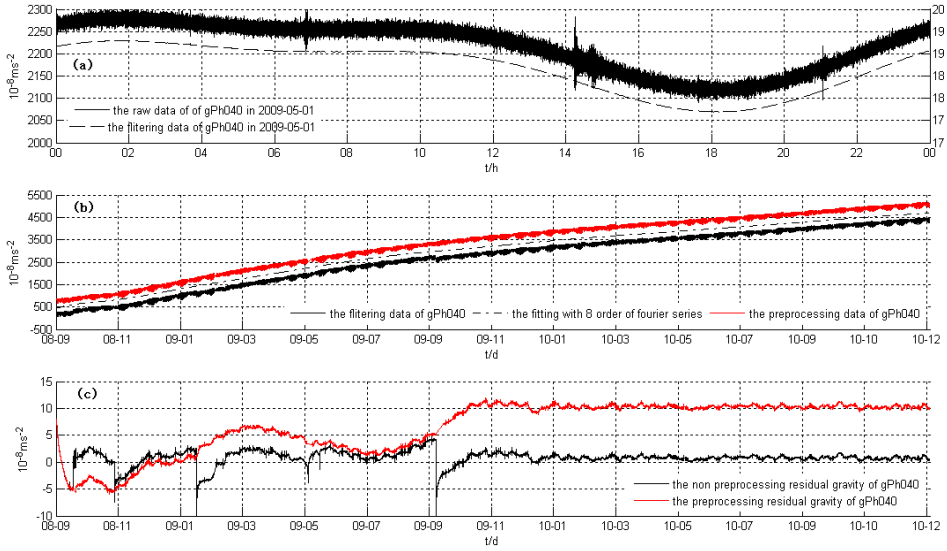


Fig. 1. The data preprocessing of gPh040 with Fourier analysis.
a) The raw data of gPh040 with 1 Hz (solid line), and the filtering data of gPh040 with 1 circle per minute (dotted line) at 2009-05-01; b) The filtering data (black line), the preprocessing data (red line) and the drift fitting by 8 order of Fourier series; c) The non preprocessing residual (black line) and preprocessing residual gravity (red line) of gPh040.

Based on the continuous drift of spring gravimeter and the gravity variation caused by natural environment, this work firstly filtered the sampling data at 1 Hz of gPh040 using ideal low pass filter [10]. Then the minute sampling gravity observation data were obtained by calibrating transformation. High order Fourier series were utilized to simulate the spring gravimeter drift after amendment of tides (see tides included). The tide amendment of observation data and their drift amendment by Fourier series fitting were performed. The residual should also be a continuous function and the variation could not exceed 100×10^{-8} ms^{-2}. The pre-processing experience of superconducting gravimeter was used for reference again [11], the accuracy and efficiency of data pre-processing would be improved by time sequence amendment of the residual after drift amendment. The dash lines in Fig. 1 (b) shows the eight order Fourier series fitting drift in this work.

In the continuous gravity observation from Sep. 2008 to Jan. 2011, the gradual recovering drift which was resulted from the external factors such as power cut, lightning stroke, and strong shock and exceeded $5\text{-}10\times10^{-8}$ ms^{-2} was hardly to distinguish by eyes because of the cover up of drift and solid earth tides under the original observation data. This work could distinguish well and further modify these errors due to the non-environment factors during observation process by Fourier analysis method.

3.3. Analysis and Amendment of Tides

Based on the observation data pre-processing of gPh040, the international two reconcile and analysis software VAV03 and ETERNA34 were used to do the tidal analysis [12], obtain the main tidal parameter, and confirm the air press admittance value and white noise level in meter observation environment with combination of observation air pressure data at the same station in this work. The gPh040 observation accuracy and stability were weighed by the time variation of meter drift rate and the time variation consequence of the highest accuracy wave tidal factor M2. The analysis results are shown as Table 1 and Table 2.

Table 1. Harmonic analytical results and their comparison of 8 waves with VAV03 and ETERNA34.

Wave group name	VAV reconcile and analysis results				ETERNA reconcile and analysis results			
	Tidal factor	Mean square error	Phase position	Mean square error	Tidal factor	Mean square error	Phase position	Mean square error
Q1	1.17007	0.00079	0.350	0.039	1.16928	0.00173	0.314	0.085
O1	1.16725	0.00016	0.190	0.008	1.16705	0.00036	0.180	0.018
P1	1.16090	0.00039	-0.099	0.018	1.15943	0.00088	-0.039	0.046
K1	1.14639	0.00011	0.071	0.006	1.14655	0.00028	0.086	0.014
N2	1.16529	0.00039	0.041	0.019	1.16598	0.00063	0.025	0.031
M2	1.16374	0.00008	0.086	0.004	1.16375	0.00013	0.088	0.006
S2	1.16328	0.00025	-0.024	0.016	1.16311	0.00028	-0.038	0.015
K2	1.16421	0.00058	0.140	0.028	1.16468	0.00085	0.190	0.042

The reconciling and analysis results of the former air pressure observation at the same station indicate that the errors of tidal factors of eight main tides are all better than ±0.8 ‰. And the mean square error order of the most accurate M2 tide is only 1/10 of the total level. Compared with the analysis result of high accurate superconducting gravimeter SGC053 [13], the mean square error is only twice than that of SGC053. Its phase position hysteresis varies at around 0° and the mean square error totally better than ±0.08°. This is revealing that although the observation accuracy of gPh040 is slightly lower than that of superconducting gravimeter, the gPh040 spring gravimeter could still provide excellent observation of gravity solid earth tide. What's more, the environment white noise level of gPh040 located in the cave is only $\pm 0.3\times10^{-8}$ ms^{-2}.This cave provides good observation environment for observing the impact of external factors such as air pressure on the gravity.

At the same time, it can be seen from the drift rate time variation and M2 tidal factor time sequence variation that the total drift rate of gPh040 is not only about 300×10^{-8} ms^{-2}/M, but also decreases gradually. But the tidal factor time sequence variation range is only 0.003 (relative variation of tidal factor is about 0.2 %), indicating the data of gPh040 gravimeter is stable in the former period and highly reliable.

The time series of the drift rate and the δ_{M2} on gPh040 are shown in Fig.2.

Table 2. The atmospheric pressure admittance and white noise level.

Analysis method	Air pressure admittance value ($10^{-8}ms^{-2}$/mbar)	White noise Level ($10^{-8}ms^{-}$)
VAV analysis	-0.269±0.0107	±0.28
ETERNA analysis	-0.265±0.0035	±0.35

Considering the Wujiahe seismic station is located inland, VAV03 tidal analysis was adopted in the tidal amendment to obtain the resultant tide. The tide-generating potential containing 1200 tidal wave component inferred by Tamura was used and the gravity variation caused by the resultant tide (solid earth tide and sea tide) in the pre-processing observation of gPh040 gravimeter was taken out. The gravity residual time sequence of Wujiahe seismic station is shown in Fig. 3 (a).

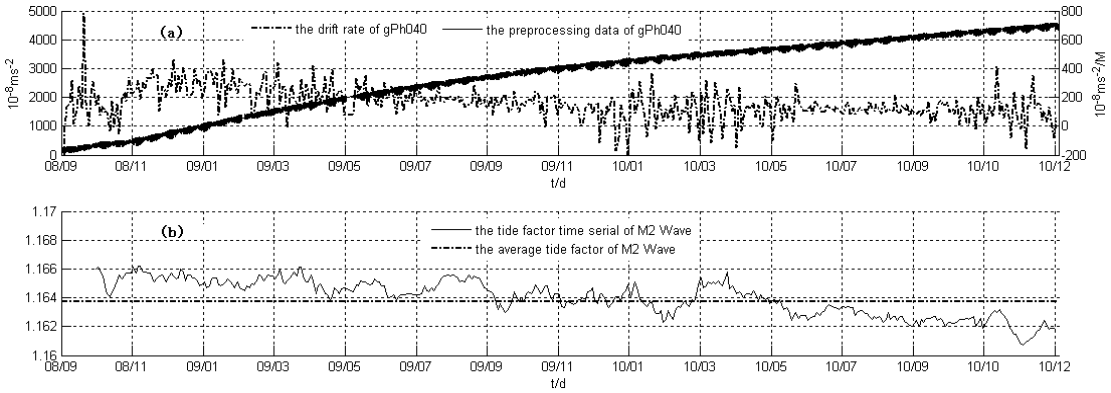


Fig. 2. The time series of the drift rate and the δ_{M2} on gPh040. (a) The time series of the preprocessed data and the drift rate on gPh040.(b) The average of δ_{M2} and the time series of the δ_{M2} on gPh040.

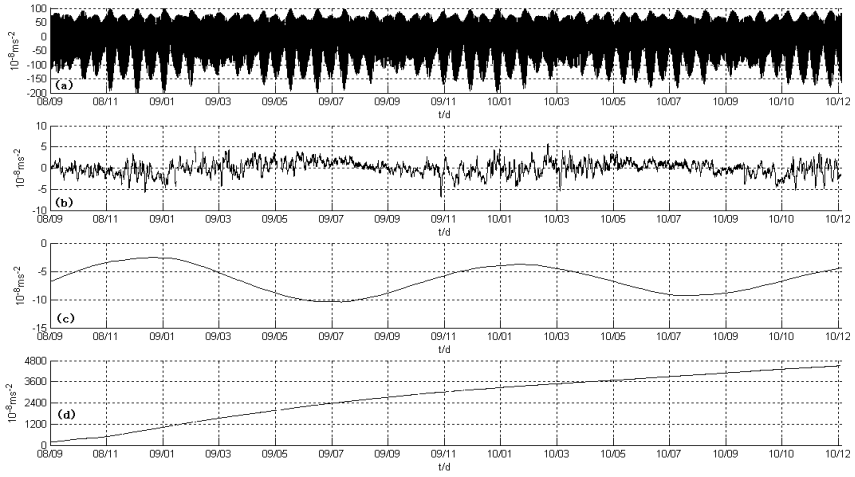


Fig. 3. Some correction and the residual of gPh040. (a) The synthetic gravity tides by VAV03 model; (b) The time series after air pressure correction; (c) The time series after polar correction; (d) The gravity residual series after correction of (a–c).

3.4. Polar Motion Amendment

The day sampling data are downloaded from International Earth Rotation Serve (IERS) website and used for observation data of calculating polar motion gravity effect. Then the linear function is used as interpolating hour value and the following equations are adopted for amendment of polar gravity effect [14]:

$$\Delta g_{pol} = -\delta_{pol}\omega^2 r \sin 2\theta[\cos(m_1\lambda) - \sin(m_2\lambda)] \quad (4)$$

where m_1 and m_2 are two parameters describing polar motion, m_1 points to meridian line direction which is east longitude 90°, (θ， λ) is the longitude and latitude of the station. The gravity effect is caused by the polar motion calculated by the equation. The gravity residual amendment value is $-\delta_g$. In this equation, tidal factor δ_{pol} is 1.16, the earth rotation angular speed ω is 7.292115×10^{-5} rad/s, and the radius of earth r is 6378137 m. The calculated results are shown in Fig. 3 (c).

3.5. Air Pressure Amendment

The gravity variation caused by atmosphere substances variation could be divided into the direct attraction impact of atmosphere load and the indirect impact generated from the atmosphere load caused by the earth's crust and sea level variation. The main parameter of measuring the effect of air pressure on a station is air pressure admittance value (shown as Table 1). In this work, the weighed mean air pressure admittance value α=-0.267±0.002×10^{-8} ms^{-2}/mbar at this station is used, which is calculated by the two reconcile and analysis methods. The air pressure amendment equation is as follows:

$$\Delta g_{air} = -\alpha(p - p_n), \quad (5)$$

where P is the time observation air pressure observation value (unit: mbar), P_n is the normal air pressure value, which equals to 900.065 mbar. The air pressure data and their amendment values are shown in Fig. 3(b).

The amendment using the resultant tide confirmed by observation data, air pressure data observed at the same station, and the polar motion data published by IERS has shown that, beside the influence of resultant tide (±150×10^{-8} ms^{-2}), air pressure (±5×10^{-8} ms^{-2}) and polar motion amendment (±8×10^{-8} ms^{-2}), the biggest impact factor is still the spring drift. Therefore, the drift amendment must be done before extracting the influence of seasonal factors.

4. Comparison between Drift Amendment and Residual Time Sequence

The elastic system of gPhone gravimeter is composed of low drift metalized zero-length spring system. The factors such as elastic hysteresis, creep, after elastic effect, the decade, the temperature, and the pressure load of spring in gravimeter elastic system must be considered if simulating the spring gravity drift. Although there are lots of factors influences the spring, the drift of spring is continuous. In this work, two methods were chosen to simulate the spring drift, and the global water load model and the underground water data were used to check the seasonal variation of residual time sequence.

4.1. Global Earth and Water Model (CPC and GLDAS)

CPC (Climate Prediction Center) is a global land water model provided by Climatic Prediction Center of NOAA U. S. A., which is the 0.5o ×0.5o soil humidity network data formed by considering the factors of soil humidity, temperature, and water fall. The temporal resolution is 1 month. Their data reflect the soil humidity data of the global land. GLDAS (global land data assimilation systems) is a global land data fusion system provided by CSR laboratory of NASA U. S. A., which constrain and simulate the ground water condition using new generation ground and space observation data. The spatial resolution of this modal is 1°×1°, and the temporal resolution is 1 month. The land water is consisting of soil water, underground water, and snow water, but without the perpetual water content variation under ice.

When calculating the influence of global water on gPh040, the equivalent water height of each grid point in the global land water model is h, the load gravity influence Lg(θ, λ) can be calculated by Green's function integral formula. θ, λ are correspondingly the earth latitude and longitude. The calculating formula is as follows [15]:

$$Lg(\theta,\lambda) = R^2\rho\iint_s G(\psi)h(\theta',\lambda')\sin\theta' d\theta' d\lambda', \quad (6)$$

where R is the mean radius of earth, θ', λ' are the integral grid point coordinates, ψ is the spherical angle distance between the station and grid point, S is the entire land area.

4.2. Relative Analysis of Two Types of Drift Fitting Method

The first method is provided by Riccardi et al (2011) [3], the observation data are firstly drift amended linearly by one order, and then the residual are drift amended by high order polynomial fitting. The second method is the direct fitting drift (see section 2) using the Fourier analysis method proposed by our work. Considered the above amendments, the residual time consequence is mainly consisting of the influence of drift and water load. After analysis of the underground water level data of Wujiahe seismic station and the gPh040 gravimeter data after deduct of the residual time consequence, and the results are as Table 3 and Table 4.

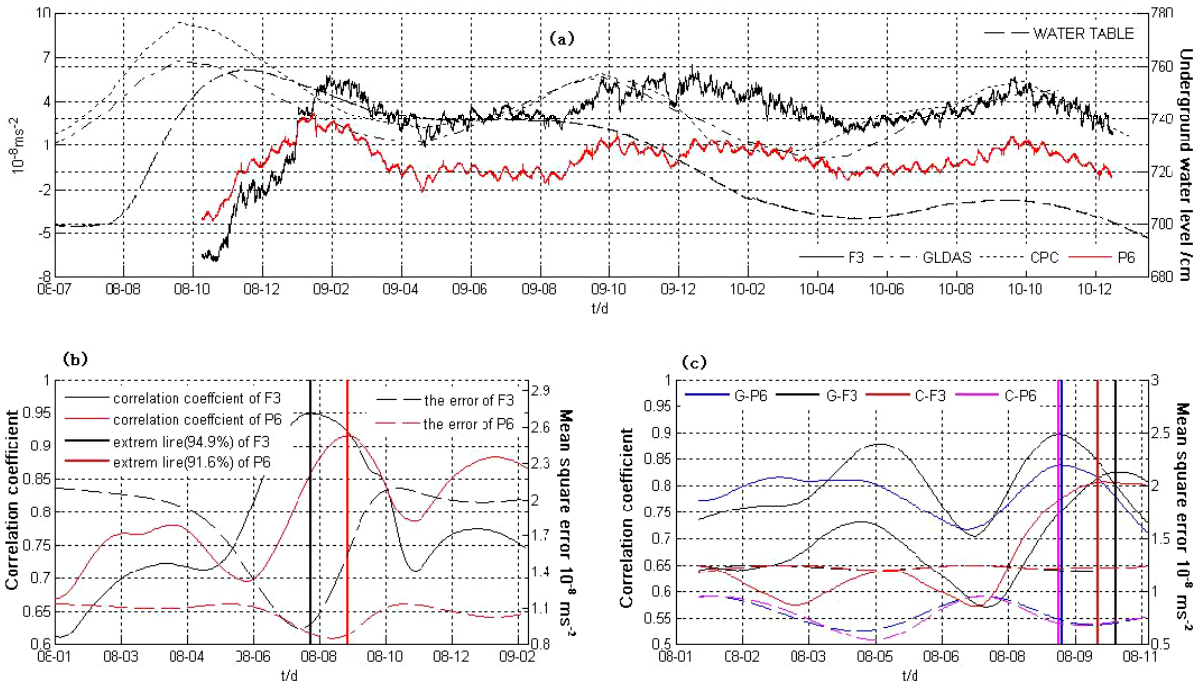


Fig. 4. The time series and correlated analysis between the residual of gPh040 with 3 order Fourier series and 6 order polynomial and the gravity change with CPC and GLDAS. (a) the time series of the table ground and the gravity effect by the global model of GLDAS and CPC; (b) The time series of the middle error and correlation coefficient between the ground table and F3, P6. The start point is 2008-01-01. The windows length is the length of F3 and F6. The step is 1 day. (c) The time series of the middle error and correlation coefficient between GLDAS, CPC, F3 and P6 by (b). The solid line in (b) and (c) represents the correlation coefficient. The dotted line indicates that the associated error analysis. Vertical lines represent extreme line.

Table 3. The table of the correlation analysis (hourly).

Model	Proportionality coefficient	Correlation coefficient	Mean square error	Phase potion days
W-F1	1.911	0.952	11.873	34
W-F2	0.151	0.927	1.277	91
W-F3	0.155	0.949	0.972	77
W-F4	0.097	0.892	1.039	82
W-F5	0.093	0.891	1.085	82
W-P4	0.191	0.868	2.127	-79
W-P5	0.079	0.897	0.929	66
W-P6	0.094	0.916	0.874	45
W-P7	0.055	0.865	0.708	37
W-P8	0.038	0.855	0.557	48

Table 4. The correlation analysis between the residual and the global model (daily statistical results) *

Model	Proportionality coefficient	Correlation coefficient	Mean square error	Phase delay
C-F3	0.126	0.806	1.225	81
C-P6	0.350	0.896	0.701	107
G-F3	0.237	0.825	1.184	68
G-P6	0.376	0.838	0.729	105

*Notes: The table only considers the results that have the smallest mean square of phase delay and the biggest coefficient of association in the 2-3 months. In the column of model, W is water table, F is Fourier series, P is polynomial, C is CPC global land water model and G is GLDAS global land water model. CPC and GLDAS used the month water load model and linearly interpolating each day's gravity effect, and analysis the whole day residual time sequence value and global model interpolating value.

The statistical results (Table 3 and Table 4) show that beside the Fourier one order and fore order polynomial fitting method, the other phase position of drift amendment methods are all delayed by 2-3 months. When the Fourier series is fixed as 3-order or the polynomial fitting is fixed as 6-order, the

dependency of the two amendment methods exceeds 90 %. This analysis result is basically the same as the global model analysis results (the dependency exceeds 80 %). At the same time, the correlation coefficients calculated by Fourier series drift amendment method are all larger than those of polynomial fitting. Therefore, the 3-order Fourier series (F3 for short) and 6-order polynomial fitting (P6 for short) could eliminate the influence of drift on the spring gravimeter and extract the gravity signal variation caused by underground water level variation (fitting equations are shown in Table 5).

Table 5. The Fitting Function of 3-order Fourier series and 6-order Polynomial *

Fitting method	Fitting times	Fitting equations
F3	1	$g_{drift}=a_0+a_1cos(\omega_0 t_i)+a_2cos(2\omega_0 t_i)+a_3cos(3\omega_0 t_i)$ $+ b_1sin(\omega_0 t_i)+b_2sin(2\omega_0 t_i)+b_3sin(3\omega_0 t_i)$ $\omega_0=0.00015839;\ a_1=2775.5746;\ a_2=-476.0818;\ a_3=36.1102;$ $b_1=-181.1816;\ b_2=555.6707;\ b_3=115.3710;$
P6	1	$g_{drift}=kt_i+b; k=0.2122; b=591.38;$
	2	$g_{drift}=a_0+a_1t+a_2t^2+a_3t^3+a_4t^4+a_5t^5+a_5t^6;$ $a_0=-408.97; a_1=-0.0523; a_2=7.16\times10^{-5}; a_3=-1.156\times10^{-8};$ $a_4=7.79\times10^{-13}; a_5=-2.488\times10^{-17}; a_6=3.1095\times10^{-22};$

*Notes: Fourier series can calculated the drift curve in one time, while polynomial fitting method firstly uses 1-order polynomial to fit, and then use 6-order polynomial to fit again for the residual time consequence.

It can be seen from the time consequence curves in Table 4 (a) that the residual time consequence of the two drift amendment methods shows obvious fluctuate phenomenon. Compared with the time consequence of underground water level, the underground water level raised up for more than 60 mm in the four months started at Aug. 2008. And the gravity residual was lifted as well from Nov. 2008 to Mar. 2009. Compared with the global water load model, the variation of underground water level is seasonal, and the gravity residual time consequence of gPh040 after drift amendment has an obvious the same variation rules.

It is shown in the time consequence of correlation coefficient and mean square error that the three water models express the seasonal variation of water migration, and the gravity hysteresis variation caused by this water seasonal variation. Moreover, the mean square error reaches its lowest value when the correlation coefficient is the largest, and the correlation of local water level variation is superior obvirously than the global load model. This indicates that the global water load model can be used to restrain the seasonal factors impact of gravity variation. But the local water level variation can be used to amend the contribution of the gravity variation in this area more accurately.

4.3. Calculation and Comparison of Gravity Impact factor of Underground Water

Based on the equations proposed by Torge et al. (1989) [16-20], Bouguer plate model could be used to describe the influence of underground water level and the soil gap water content time variation on the gravity:

$$\delta_{gw} = 2\pi G\rho_w P\delta H = 0.42P\delta H\,, \tag{7}$$

where the unit of underground water level gravity variation δ_{gw} is 10-8ms^{-2}, G is the gravitation constant, ρ_w is the water density 1×103 kgm^{-3}, the unit of soil gap water content P is %, and the unit of water level variation δH is cm. Considering the drill strain gap water pressure is used in this underground water observation, the soil gap water content is about 10%-15 %. The theoretical impact factor of Wujiahe area underground water to gravity calculated by equation (7) is 0.21~0.04×10-8 ms^{-2}/cm. This theoretical range is basically the same as the real observation result (the gap water content using underground water level estimated to be 25 %-35 %). Fourier analysis method is more reliable because of consideration of fitting correlation.

5. Conclusions

In this work, the continuous gravity observation data in Wujiahe seismic station during two and a half years were used, and Fourier series and polynomial fitting methods were adopted. The seasonal variation of gravity has been extracted with utilizing air pressure and underground water level observation at the same station, and GLDAS, CPC global land water model. The result shows that the gPhone has been working stably during the period from Sep. 2008 to Jan. 2011 after data pre-processing using Fourier analysis assisted by conducting gravimeter pro-processing method. The observation accuracy of this meter could reach half of that of the conducting gravimeter under the white noise level of 0.3×10^{-8}ms^{-2}. The pressure admittance value is -0.267±0.002×10^{-8} ms^{-2}/mbar.

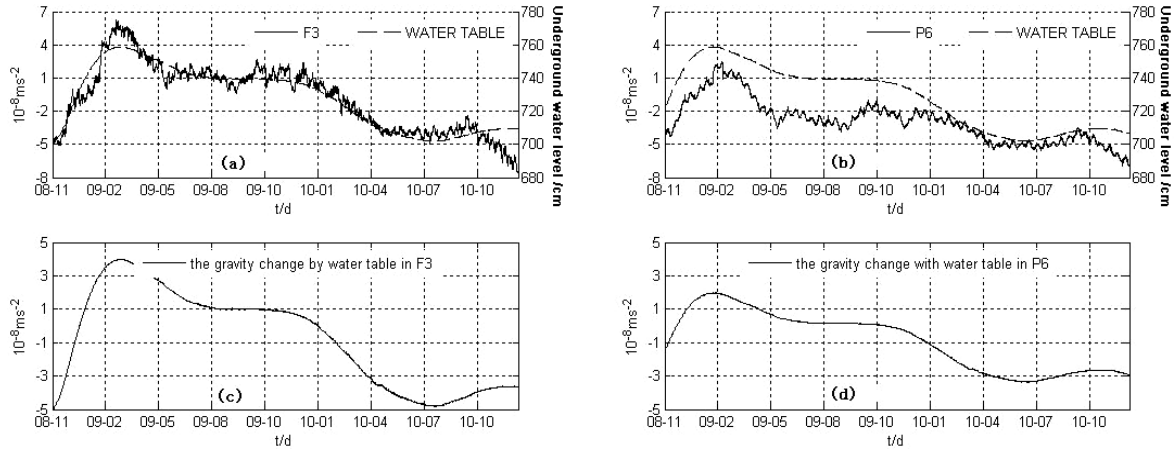


Fig. 5. The relationship between the residual gravity and water table and the gravity change by water table. (a) The residual gravity corrected by F3 and the water table corrected by phase lag; (b) the residual gravity corrected by P6 and the water corrected by phase lag; (c) the water table correction with $0.153\times10^{-8}ms^{-2}$/mm; (d) the water table correction with $0.093\times10^{-8}ms^{-2}$/mm.

The amendment using resultant tide from observation data, air pressure data at the same station, and the polar motion data has shown that, beside the effect of resultant tide ($\pm300\times10^{-8}ms^{-2}$), air pressure ($\pm5\times10^{-8}ms^{-2}$) and polar motion ($\pm7\times10^{-8}ms^{-2}$), the most dominant influence factor is the spring continuous drift. It has been analyzed that the positive direction rate of Wujiahe seismic station spring is approximately $300\times10^{-8}ms^{-2}$/M.

In the premise of hypothesis that the drift of spring gravimeter and the gravity non-tidal variation should be a continuous process, the polynomial fitting method was used for comparison in this work. The efficiency of Fourier series fitting drift has been verified by using hill and underground water level data in Wujiahe seismic station and the two global land water models (GLDAS and CPC). The result shows an obvious seasonal rule could be reflected by polynomial and Fourier series fitting drift amendment methods, when comparing with the global land water model or the underground water level observation. The relative analysis indicates the correlation between them is more than 80 %. The underground water level amendment residual time consequence shows that the underground water level gravity influence impact factors obtained by two kinds of methods are almost the same as theoretical value. But the correlation of 95 % between Fourier analysis result and underground water level observation indicates that the spring gravimeter continuous drift fitted and the seasonal variation extracted by Fourier series are more reliable than those of polynomial analysis. The gravity influence of Wujiahe seismic station underground water level is approximately $\pm5\times10^{-8}$ ms^{-2}, and the gap water content of Wujiahe area is approximately 25 %-35 %.

Compared with polynomial fitting, the Fourier analysis could also fit the continuous drift of spring gravimeter. The advantage of this method is not only once time molding, but the effect is also superior to those of polynomial fitting. The former method and underground water data could be used not only to extract the gravity variation caused by seasonal underground water level variation, but also to extract the gravity variation caused by non-seasonal factors. This method provides a new method and way to extract the contribution of seasonal underground water from the gPhone continuous observation data and the influence of non-seasonal factors.

Acknowledgements

The work was supported by the Fund of National Natural Science Foundation (41004030; 40974015), the National Network of centers of gravity operating funds (201 101 008), China Seismological Bureau, director of the Earthquake Research Institute Foundation (IS200956041).

References

[1]. Tapley B. D., Bettadpur S., Ries J. C., Thompson P. F., Watkins M. M., GRACE measurements of mass variability in the Earth system, *Science*, Vol. 305, Issue 23, 2004, pp. 503-505.

[2]. Imanishi Y., Sato T., Higashi T., Sun W. K, Okubo S., A network of superconducting gravimeters detects submicrogal coseismic gravity changes, *Science*, Vol. 306, Issue 5695, 2006, pp. 476-478.

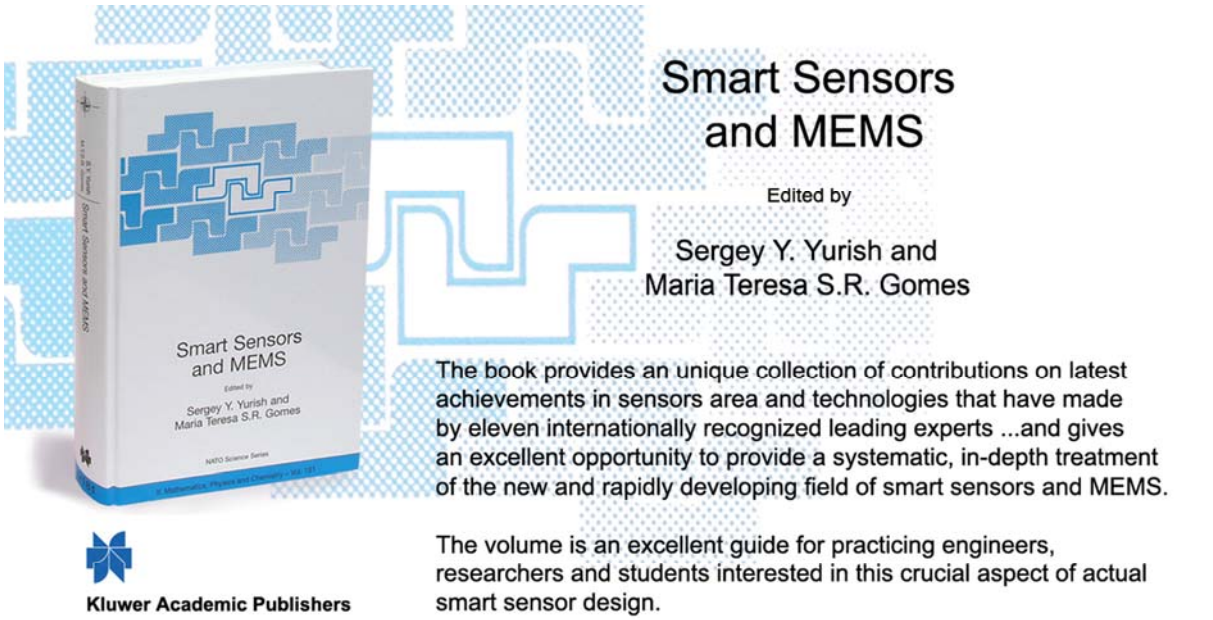
[3]. Sun W., Wang Q., Li H., Wang Y., Okubo S., Shao D. S., Fu G. Y., Gravity and GPS measurements reveal mass loss beneath the Tibetan Plateau Geodetic evidence of increasing crustal thickness, *Geophysical Research Letters*, 2009, Vol. 36, L02303.

[4]. Sun W., Wang Q., Li H., Wang Y., Okubo S., A reinvestigation of crustal thickness in the Tibetan Plateau using absolute gravity, GPS and GRACE data, *Terr Atmos Ocean*, Vol. 22, Issue 2, 2011, pp. 109-119.

[5]. He Ping Sun, Takemoto S., Hsu H.-T., Higashi T., Mukai A., Precise tidal gravity recorded with

superconducting gravimeters at stations Wuhan (China) and Kyoto (Japan), *Journal of Geodesy*, Vol. 74, Issue 10, 2001, pp. 720-729.
[6]. Camp M. V., Francis O., Is the instrumental drift of superconducting gravimeters a linear or exponential function of time, *Journal of Geodynamics,* Vol. 81, 2007, pp. 337-344.
[7]. Riccardi U., Rosat S., Hinderer J., Comparison of the Micro-g LaCoste gPhone-054 spring gravimeter and the GWR-C026 superconducting gravimeter in Strashourg (France) using a 300-day time series, *Metrologia*, Vol. 48, 2011, pp. 28-39.
[8]. Kang K. X., Li H., Peng P., Hao H. T., Wei J., Seasonal variations in hydrological influences on gravity measurements using gPhone, *Terr. Atmos. Ocean*, Vol. 22, 2011, pp. 157-168.
[9]. Xing Lelin, Li Hui, Xia Zhengchao, Hao Xinghua, Hao Hongtao, Liu Ziwei, Study on zero drift characteristics of CG-5 gravimeter, *Acta Seismologica Sinica*, Vol. 32, Issue 3, 2010, pp. 369-373.
[10]. Liu Ziwei, Li Hui, Hao Hongtao, Wei Jin, Xing Lelin, Analysis of observations of superconducting gravimeter SG-053, *Journal of Geodesy and Geodynamics*, Vol. 30, Issue 6, 2010, pp. 157-160.
[11]. Xu Jianqiao, Theory and analysis method of gravity solid tidal - analysis and dispose of Wuhan station superconducting gravimeter observation data, Doctor's Thesis, *Institute of Geodesy and Geophysics*, China, 1997.
[12]. Tian Guie, Chen Xiaodongm Sun Heping, Chen Guang, Song Lijie, Liu Nannan, Comparison and investigation of VAV and ETERNA tidal analysis methods, *Journal of Geodesy and Geodynamics*, Vol. 29, Issue 2, 2009, pp. 96-99.
[13]. Wei Jin, Li Hui, Liu Ziwei, Kang Kaixuan, Noise level measurement of SG-053 with MLE, *Journal of Geodesy and Geodynamics*, Vol. 31, Issue 3, 2011, pp. 69-74.
[14]. Chen X. D., Kroner C., Sun H. P., Abe M., Zhou J. C., Yan H. M., Wziontek H., Determination of gravimetric parameters of the gravity pole tide using observations recorded with superconducting gravimeters, *Journal of Geodynamics*, Vol. 48, 2009, pp. 348-353.
[15]. Zhou Jiangcun, Sun Heping, Xu Jianqiao, Validating global hydrological models by ground and space gravimetry, *Chinese Sci. Bull*., Vol. 54, Issue 9, 2009, pp. 1534-1542.
[16]. Torge W., Gravimetry, *Walter de Gruyter,* Berlin, New York, 1989.
[17]. Zerbini S., Raicich F., Richter B., Gorini V., Errico M., Hydrological signals in height and gravity in northeastern Italy inferred from principal components analysis, *Journal of Geodynamics*, Vol. 49, 2010, pp. 190-204.
[18]. Hasan S., Peter A. T., Boll J., Kroner C., Modeling the hydrological effect on local gravity at Moxa, *Journal of Hydrometeorology*, Vol. 7, 2005, pp. 346-354.
[19]. Abe M., Takemoto S., Fukuda Y., Higashi T., Imanishi Y., Iwano S., Ogasawara S., Kobayashi Y., Dwipa S., Kusuma D., Hydrological effects on the superconducting gravimeter observation in Banding, *Journal of Geodynamics*, Vol. 41, 2006, pp. 288-295.
[20]. Neumeyer J., Barthelmes F., Dierks O., Flechtner F., Harnisch M., Harnisch G., Hinderer J., Imanishi Y., Kroner C., Meurers B., Petrovic S., Reigber Ch., Schmidt R., Schwintzer P., Heping Sun, Virtanen H., Combination of temporal gravity variations resulting from superconducting gravimeter (SG) recordings, GRACE satellite observations and global hydrology models, *Journal of Geodesy*, Vol. 79, Issue 10-11, 2006, pp. 573-585.

2014 Copyright ©, International Frequency Sensor Association (IFSA) Publishing, S. L. All rights reserved. (http://www.sensorsportal.com)







IEEE International Workshop on Metrology for Aerospace

Benevento, Italy, June 4 - 5, 2015

HONORARY CHAIR
Marina Ruggieri, Italy

GENERAL CHAIRS
Pasquale Daponte, Italy
Robert Rassa, US

TECHNICAL PROGRAM CO-CHAIRS
Stephen Dyer, US
Alfonso Farina, Italy

PUBLICATION CHAIR
Ernestina Cianca, Italy

TREASURY CHAIR
Cosimo Stallo, Italy

INTERNATIONAL PROGRAM COMMITTEE
Domenico Acierno, Italy
Carlo Albanese, Italy
Giovanni Betta, Italy
Erik P. Blasch, US
Paolo Carbone, Italy
Luigi Carrino, Italy
Goutam Chattopadhyay, US
Stefano Debei, Italy
Murat Efe, Turkey
Pietro Ferraro, Italy
Jesus Garcia, Spain
Domenico Giunta, Netherlands
Maria S. Greco, Italy
Richard Hochberg, US
Satoshi Ikezawa, Japan
Stephen Johnson, US
Karel Kudela, Slovak Rep.
Chin E. Lin, Taiwan
Walter Matta, Italy
Daniele Mortari, US
Aldo Napoli, France
Pavel Paces, Czech
Jacek Pieniazek, Poland
Vasily Popovich, Russia
Helena G. Ramos, Portugal
Artur L. Ribeiro, Portugal
Roberto Sabatini, Australia
Nicolas Sklavos, Greece
Patrizia Tavella, Italy
Fabrizio Francesco Vinaccia, Italy
Graham Wild, Australia
Ho-Soon Yang, Republic of Korea
Mark Yeary, University of Oklahoma, US
David Zucconi, Italy

LOCAL COMMITTEE
Pasquale Arpaia, Italy
Luca De Vito, Italy
Gianluca Mazzilli, Italy
Francesco Picariello, Italy
Sergio Rapuano, Italy
Silvia Ullo, Italy
Judy Scharmann (IEEE AESS Executive Assistant)

LOCAL ARRANGEMENTS

ATHENA SRL

ABOUT THE WORKSHOP

MetroAeroSpace aims to gather people who work in developing instrumentation and measurement methods for aerospace. Attention is paid, but not limited to, new technology for metrology-assisted production in aerospace industry, aircraft component measurement, sensors and associated signal conditioning for aerospace, and calibration methods for electronic test and measurement for aerospace.

WORKSHOP TOPICS

The main topics include, but are not limited to:

- Electronic instrumentation for aerospace
- Automatic test equipment for aerospace
- Sensors and sensor systems for aerospace applications
- Wireless sensor networks in aerospace
- Attitude - and heading - reference systems
- Monitoring systems in aerospace
- Metrology for navigation and precise positioning

PAPER SUBMISSION

Paper submission will be handled electronically, through the submission page set up on the conference web page: **www.metroaerospace.org**

The best contributions will be awarded, including the Best Student Paper Award and the Best Paper authored and presented by a woman.

Special sessions will be organized on specific topics, see online at:

www.metroaerospace.org/index.php/program/special-session

IMPORTANT DATES

- **January 11, 2015** – Submission of Extended Abstract
- **March 1, 2015** – Notification of Acceptance
- **April 19, 2015** – Submission of Final Paper

BENEVENTO

Benevento, due to the Santa Sofia's Church with its Cloister, has been part of UNESCO World Heritage Sites as "*Longobards in Italy. Places of the power*".



CONTACT US

www.metroaerospace.org

info@metroaerospace.org

With the endorsement of

Università degli Studi del Sannio

DAC Distretto Aerospaziale della Campania